Polymer 50 (2009) 2209–2219

Contents lists available at ScienceDirect

Polymer

journal homepage: www.elsevier.com/locate/polymer

Fluorescence study of the dynamics of a star-shaped poly(ε-caprolactone)s in THF: A comparison with a star-shaped poly(L-lactide)s

Martin Danko [a,b,*], Jan Libiszowski [a], Marian Wolszczak [c], Dusan Racko [b], Andrzej Duda [a]

[a] Centre of Molecular and Macromolecular Studies, Polish Academy of Sciences, Sienkiewicza 112, 90-363 Lodz, Poland
[b] Polymer Institute, Centre of Excellence GLYCOMED, Slovak Academy of Sciences, Dubravska cesta 9, 842 36 Bratislava, Slovakia
[c] Institute of Applied Radiation Chemistry, Technical University, Wroblewskiego 15, 93-590 Lodz, Poland

ARTICLE INFO

Article history:
Received 31 October 2008
Received in revised form
5 March 2009
Accepted 16 March 2009
Available online 25 March 2009

Keywords:
Fluorescence
Star-shaped
Poly(ε-caprolactone)

ABSTRACT

Molecular dynamics of 2-, 4- and 6-arm star-shaped poly(ε-caprolactone)s (PCLs) functionalized with pyrene at all chain ends followed by excimer formation were investigated in THF as a solvent. Dilute solutions (10^{-8} to 10^{-6} mol L^{-1}) of these polymers revealed excimer emission due to the intramolecular cyclization, proceeding via chain end interaction. Time-resolved fluorescence measurements of star-shaped PCLs showed complex decay profiles of monomer and excimer fluorescence. An intensity rise component of decay profiles monitored in excimer region (500 nm) was observed for star-shaped polymers due to dynamic formation of excimers. Dipyrene–PCL (2-arm) also showed partial formation of static pyrene excimers as followed from measurement of excitation spectra at ambient temperature in THF. Excimer intensity of di- and four pyrene–telechelic PCLs was found to be comparable with that of di- and four pyrene–telechelic polylactide (PLA) polyesters having similar molar masses. 6-Arm PCL showed depressed excimer formation with regard to 6-arm PLA under the otherwise identical conditions contrary to the conclusion expected from the higher flexibility of the PCL chain. Eventually, molecular dynamic simulations showed that possible explanation can be related to different conformations of 6-arm PLA versus PCL stars.

1. Introduction

Poly(ε-caprolactone) (PCL) is a synthetic biodegradable aliphatic polyester, that attracted considerable research attention in recent years, particularly in the specialty biomedical areas of controlled-release drug delivery systems, absorbable surgical sutures, nerve guides, and three-dimensional scaffolds for use in tissue engineering [1–3]. Macromolecular engineering offers methods such as controlled radical polymerizations (atom-transfer radical polymerization (ATRP), RAFT, nitroxide-mediated radical polymerization (NMRP)) or ring-opening polymerizations (ROPs) of cyclic lactones developed in recent years for precise, controlled synthesis of polymers with strictly designed structure like branched, hyperbranched, star-shaped and dendritic macromolecules. Properties of such polymers do not only depend on their chemical composition, but depend also on their topology [4]. Thus, understanding the behavior of these polymers in different media is desired. It is known that macromolecular architecture affects the properties of polymers, including rheological behavior and properties in solution as well as displayed peculiar morphologies, thermal properties and different degradability.

The best method for aliphatic polyester synthesis is a ring-opening polymerization of cyclic esters initiated with covalent metal alkoxides or carboxylates [5–7]. Perhaps, the most convenient initiating system for synthesis of the branched aliphatic polyester consists of a mixture of tin octoate [tin(II) bis-(2-ethyl hexanoate), $Sn(Oct)_2$] and a polyol or polyamine of the corresponding topology [8–18]. Recently, the mechanism of this polymerization has been elucidated [18–22]. From the family of polyesters, different star polylactides (PLAs) [17,23], polydioxanones [24] or PCLs [17,25–27] have been synthesized and characterized. Klok et al. [17] investigated mainly the solid state properties of star-shaped PLAs, PCLs and poly(γ-*tert*-amyl-ε-caprolactone)s prepared by ring-opening polymerization using different multifunctional core co-initiators, some of them with fluorescence ability. Fréchet et al. [26,27] characterized star-shaped PCLs by fluorescence spectroscopy using a porphyrine core or functionalized chain ends with other fluorescence probes. In

* Correspondence to: M. Danko, Polymer Institute, Centre of Excellence GLYCOMED, Slovak Academy of Sciences, Dubravska cesta 9, 842 36 Bratislava, Slovakia. Tel.: +421 2 54777404; fax: +421 2 54775923.
E-mail address: upoldan@savba.sk (M. Danko).

0032-3861/$ – see front matter © 2009 Elsevier Ltd. All rights reserved.
doi:10.1016/j.polymer.2009.03.027

a separate series of papers the authors describe the thermal properties or biodegradability of polymeric materials made of star-shaped polyesters [23–25]. On the other hand, the solution properties of functional star-shaped polyesters with respect to arm molecular dynamics can possibly give a better understanding of their behavior in different applications [15,16,28,29]. Generally, such behavior has been investigated for linear (including ditelechelic polymers, such as polystyrene [30–32], PCL) [33] or poly(ethyleneoxide) [34].

Recently, we employed the excimer formation of pyrene terminated polymer chains to monitor the molecular dynamics of star-shaped PLAs in THF solution [35]. Static as well as time-resolved fluorescence studies showed only the formation of dynamic excimers due to end-to-end cyclization. Besides, no static pyrene excimers were observed. In THF solution the polymers assumed an extended coil conformation allowing free dynamics of polymer segments. Excimer emission was low because a majority of the excited pyrenes stayed separated and decayed separately (as a monomer emission). Thus, fluorescence spectroscopy allowed us to follow the molecular dynamics of star-shaped PLA polymers in solution.

In the present article we focus on the molecular dynamics of pyrene-functionalized star-shaped 4- and 6-arm PCLs as well as linear PCLs with only mono- or difunctionalized chain ends in THF solution using static and dynamic fluorescence measurements. In addition, theoretical molecular simulations of 6-arm PCL and PLA stars were performed for a better explanation of phenomena that appeared during interpretation of data from static and time-resolved fluorescence spectroscopy for the prepared model polymers. The results obtained for star-shaped PCLs and PLAs, both with identical number of arms and average molecular weight per arm, are finally discussed.

2. Experimental part

2.1. Materials

Tin octoate (tin(II) 2-ethylhexanoate, ($Sn(Oct)_2$)) commercial product (Aldrich) employed as a co-initiator for the ring-opening polymerization of ε-caprolactone was purified by two consecutive high vacuum distillations at 140 °C/3×10^{-3} mbar. Thus purified tin octoate (99% of purity according to ^{1}H NMR) was distributed on the vacuum line directly into thin-walled vials. ε-Caprolactone (CL, Koch-Light Laboratories, England) was refluxed over CaH_2 and distributed to ampoules by distillation under reduced pressure. The purified monomer was distributed into thin-walled vials and sealed under vacuum. Di(ethylene glycol) (DEG, Aldrich, 99%) was dried with Na metal and distributed by the distillation under a reduced pressure (3×10^{-3} mbar, ≈150 °C) into the thin-walled vials. Di(pentaerythritol) (DPET, Perstorp, Sweden) was used as received. Modified DPET (m-DPET) used as a co-initiator with four hydroxy groups (Scheme 1) was prepared by a three-step synthesis from DPET using benzyl bromide as a blocking reagent as has been described elsewhere [36]. Tetrahydrofuran (THF, POCh, Gliwice, Poland, p.a. grade) was dried by keeping several days over KOH pellets, filtered off and refluxed and distilled over Na metal, degassed and stored over liquid Na/K alloy. *n*-Hexane was dried by refluxing and distilling over Na metal. Pyridine (Aldrich, 99%) was dried by keeping over KOH pellets for several days, then filtered off and distilled under reduced pressure from CaH_2 just before use. THF as a solvent for fluorescence measurements was purified by a slow distillation over Na metal, stored under argon and its spectroscopic purity was checked before use.

Ethyl 4-(1-pyrene)butanoate was prepared by esterification of 4-(1-pyrene)butanoic acid (Aldrich, used as received) with ethanol (absolute), which was used as both solvent and reagent, in the presence of small amount of sulfonic acid. Recrystallization of the crude product from *n*-hexane gave crystals of the product with m.p. 40–42 °C and the appropriate ^{1}H NMR spectra.

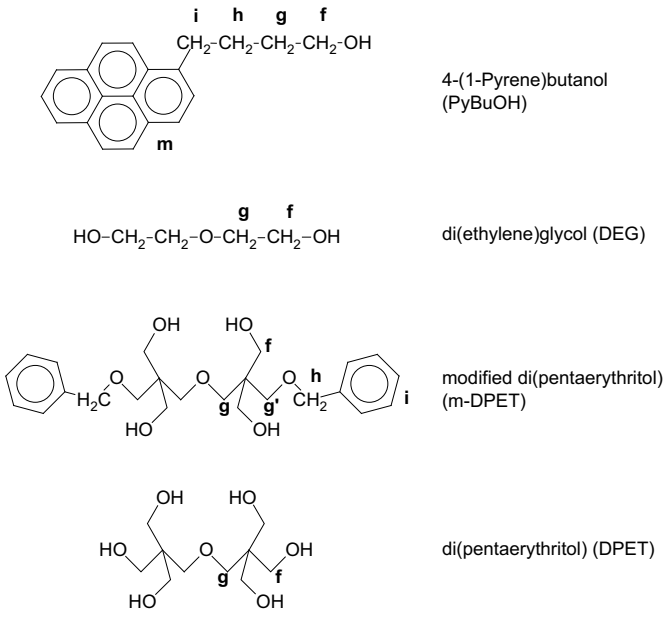

Scheme 1. Structure of hydroxyl co-initiators used for preparation of linear and star-shaped PCL polyesters.

2.2. Procedure

Preparation of star-shaped hydroxyl-terminated poly(ε-caprolactone)s (PCLs) with 2-, 4- and 6 arms was carried out by a traditional procedure in THF using $Sn(Oct)_2$ as a co-initiator following the procedures for preparation of star-shaped poly(L-lactides) described elsewhere [35,36]. DEG, DPET and m-DPET (4-OH groups) were employed as polyol co-initiators (Scheme 1).

The polymerization mixtures were prepared in sealed glass ampoules using a standard high vacuum technique. Breakseal equipped with a hammer containing the $Sn(Oct)_2$/THF solution, breakseal with CL and breakseal with dried hydroxylic co-initiator were sealed to the reacting glass vessel. Concentration of the reactants and reaction conditions are described in Table 1. The remaining amount of THF needed was distilled under vacuum into the vessel and the vessel was sealed after freezing in liquid nitrogen. The breakseals were broken and all components were mixed at room temperature. The ampoule containing the reaction mixture was placed into an oven thermostated at 80 °C for 10 h in the case of 2-arm PCL and 11 h in the case of 4-arm PCL. Monomer conversion after this time, determined by SEC, was about 80%. In the case of 6-arm PCL, the polymer was prepared using an unconventional method with an excess of hydroxylic co-initiator due to partial insolubility of the co-initiator in THF. Molar mass of the polymer was determined by SEC at various polymerization times and the polymerization was stopped after 5.5 h at a monomer conversion of 80%. All prepared polymers were separated and purified by repeated precipitation into cold methanol, filtered and dried under vacuum for several hours. Characterization of the polymers is summarized in Table 1.

A general procedure for the functionalization of hydroxyl-terminated star-shaped polymers has been described previously [35]. Briefly, to the stirred solution of 0.2 g of polymer in dried pyridine (5 mL) under the Ar atmosphere 4-(1-pyrene) butyric acid

Table 1
Reaction conditions and characterization of prepared star-shaped PCL polymers.

Polymer – no. of arms	Initiating system[a]	$[I]_0$ [mol L^{-1}]	$[col]_0$ [mol L^{-1}]	$[M]_0$ [mol L^{-1}]	M_n[c] (calc)	M_n (M_w/M_n)[d] (SEC)	M_n (NMR)
APCL-1-PB	$Sn(Oct)_2$/PyBuOH	0.005	0.062	2.0	3290	2670 (1.20)	3830
APCL-2-PB	$Sn(Oct)_2$/DEG	0.005	0.032	2.0	7230	6940 (1.14)	7010
APCL-4-PB	$Sn(Oct)_2$/m-DPET	0.005	0.016	2.0	11830	7890 (1.27)	9320
APCL-6-PB	$Sn(Oct)_2$/DPET[b]	–	–	–	–	12 040 (1.16)	17 310

[a] $Sn(Oct)_2$ – tin^{II} (2-ethylhexanoate); PyBuOH – 4-(1-pyrene) butanol; m-DPET – modified di(pentaerythritol) (see Scheme 1); DPET – di(pentaerythritol); polymerizations were performed in THF solution at 80 °C.
[b] Quasi-solution polymerization in THF at 80 °C (see Experimental part).
[c] M_n (calc) $= M_M[M]_0/[col]_0 + M_{ROH}$, calculated with 80% conversion.
[d] Calculated by multiplying molar masses from SEC with coefficient 0.68 (conversion factor) for the polystyrene standards.

chloride (5 M excess with respect to the concentration of –OH group of polymers calculated from NMR) was added. The reaction mixture was then stirred for 16 h at 80 °C. The functionalized polymer was precipitated into cold methanol, filtered and washed three times with water and twice with methanol. The yields of the vacuum dried products were 50–90%. After that, the polymers were re-precipitated from THF solution into cold *n*-heptane, filtered off and dried. The polymers were finally purified by lyophilization using benzene in order to remove the remainder *n*-heptane and carefully dried under high vacuum for several hours. Polymers purified by this way did not contain any low molecular pyrene impurities. Molar masses of the functionalized polymers were similar to those before functionalization (see Table 2) and polydispersity indexes were also kept narrow. Characteristics of functionalized star-shaped PCLs are summarized in Table 2.

In order to prepare linear PCL functionalized only on one end of polymer chain, 4-(1-pyrene) butanol was used as a hydroxylic co-initiator. Polymerization was carried out in THF at 80 °C. Polymerization mixtures were prepared in sealed glass ampoules using the standard high vacuum technique as described above. Reaction conditions are listed in Table 1. Conversion of monomer monitored by SEC was 80%. The resulting polymer was precipitated into cold methanol, filtered, washed several times with methanol, re-precipitated from THF into methanol and dried under high vacuum for several hours.

2.3. Measurements

^{1}H NMR spectra were performed on Bruker DRX 500 (500 MHz) instrument in $CDCl_3$. Residual $CHCl_3$ was used as an internal standard ($\delta = 7.26$ ppm).

Size exclusion chromatography (SEC) was performed using an Agilent Pump 1100 Series (preceded by an Agilent G1379A Degasser), set of TSK Gel G 2000 HXL and 6000 HXL columns with pore sizes 2.5×10^2 and 2.5×10^6 Å, respectively, at 30 °C. Wyatt Optilab Rex interferometric refractometer (Wyatt Technology Corp., Santa Barbara, CA) was used as detector. Methylene chloride was used as an eluent at a flow rate of 0.8 mL min^{-1}. The system was calibrated according to polystyrene standards. M_n and M_w/M_n were calculated from the experimental traces, using Wyatt ASTRAv 4.90.07 program.

UV spectra were performed on a Shimadzu 1650PC instrument. A calibration curve for determining the average molar mass of polymers from the UV spectra was constructed using ethyl 4(1-pyrenyl)butanoate in THF as a solvent in a concentration range 10^{-7} to 10^{-5} mol L^{-1}. Steady-state fluorescence spectra were recorded on Perkin–Elmer LS 50 luminescence spectrometer in a 1 cm quartz cell in right-angle arrangement at room temperature in the concentration range 10^{-8} to 10^{-6} mol L^{-1} calculated for the pyrene chromophore. Excitation and emission slits were set at 2.5 or 5 nm. The polymer samples were dissolved in THF and deaerated by bubbling with argon for 10–15 min. The excitation wavelength was 342 nm. Excitation spectra were monitored at 376 nm and 475 nm for monomer and excimer emission, respectively, in the same concentration range as for emission spectra. The excimer to monomer intensity ratio (I_E/I_M) was calculated from the intensity value of excimer band at 475 nm (I_E) divided by the intensity value of monomer band at 376 nm (I_M). Time-resolved fluorescence measurements were performed on a flash photolysis system. The instrument consists of a nitrogen laser (Laser Photonics, LN120C) providing single light pulses (337.1 nm, with duration of 300 ps and energy of 70 μJ), the detection system: monochromator Acton Research SpectraPro 275 or Bausch & Lomb, photomultiplier Hamamatsu R 3896 or 1P28 and a power supply Stanford Research System PS325. The signal output from the photomultiplier was digitized and recorded using a Tektronix TDS 680C oscilloscope and transferred via a GPIB to the computer. All measured THF solutions of polymers were carefully deaerated by the freeze–pump–thaw technique.

2.4. Theoretical molecular simulation

The structures of all the building units and corresponding monomers of 6-arm PCL and PLA star polymers, i.e. ε-caprolactone monomer or L,L-dilactide building units, the central (core) DPET unit, the ending 4-(1-pyrene)butanoyl unit, were simulated. The

Table 2
Characterizations of polymers after functionalization of –OH end groups with 4-(1-pyrene) butyric acid chloride.

Polymer – no. of arms	M_n (NMR) before func.	M_n[a] (NMR)	M_n (NMR) for arm	M_n (M_w/M_n)[b] (SEC)	I(pyr)/I(col)[c] (NMR)		Conversion of func. [%]	M_n[d] (UV)
					Calc.	Found		
APCL-1-PB	3830	3830	3560	4870 (1.18)	1	1.01	–	4220
APCL-2-PB	7010	7320	3470	8300 (1.17)	1	0.99	0.99	6530
APCL-4-PB	9320	9340	2340	9790 (1.13)	1	0.98	0.98	9170
APCL-6-PB	17 310	19 300	3180	15440 (1.19)	1	–	≈100	11 190

[a] Calculated without molar masses of end groups (270 g mol^{-1} for 4-(1-pyrene) butyric moiety).
[b] Calculated by multiplying molar masses from SEC with coefficient 0.68 (conversion factor for the polystyrene standards – SEC).
[c] Integral intensity ratio of signals **f** protons of co-initiator and **j** protons of end group (see Scheme 2 and ^{1}H NMR spectra in Fig. 1). For linear PCL with one pyrene, ratio of integral of –C**H$_2$**–O– signal of co-initiator to terminal –C**H$_2$**–OH of last caprolactone unit was calculated.
[d] Determination of average molar masses from UV spectra of polymers in 1 wt% THF solutions according to Lambert–Beer's law and using a calibration curve for ethyl 4-(1-pyrene)butanoate in THF in concentration range of 5×10^{-7}–10^{-5} mol L^{-1}. Calculated without molar masses of end groups (270 g mol^{-1} for 4-(1-pyrene) butyric moiety).

molecules were built from "sketch", i.e. a position of every atom must have been created. Next, the molecules were constructed according to the standard routine – after all atoms were present and all the chemical bonds were set, the structure was "cleaned", so that the atoms got into default respective distances and angles were adjusted according to the hybridization of orbitals. Then the geometry of the molecules was optimized by minimizing the molecular mechanics potential energy function while the geometry of the molecule adjusts also according to the steric effects. The potential energy function was described by the polymer consistent force-field (PCFF) potential energy function [37]. The energy minimization employed the Conjugate gradient method using Polak–Ribiere algorithm [38]. A convergence criterion was set to 1×10^{-3} kcal mol^{-1} Å^{-1}. The non-bonded interaction energy form included van der Waals and coulomb energy contributions as defined in PCFF. The energy cut-off for the non-bonded interactions was set to 9.5 Å. Additionally, in the case of the monomer structures, geometries have been optimized by using the extended Austin model [39] for the semi-empirical quantum mechanics, the so-called Rectife model RM1 [40] lately implemented in the MoPac2007 [41], which represented optimal level of theory from the aspect of computational costs for this problem. The obtained structures were used in the geometrical analysis of the building units or monomers respectively. Several molecular characteristics were evaluated, following Connolly's molecular volume and area (van der Waals measures) [42], ellipsoidal volume and the longest dimensions of the molecules [43].

The obtained optimized structures for the building units were used in the subsequent construction of the polymeric structures. The polymer contained six branches consisting of 20 repeat units attached through head-to-tail way. Each branch was terminated by a 4-(1-pyrene)butanoyl moiety and the branches were attached to one central unit of di(pentaerythritol). The optimized monomers were connected to each other with respect to hybridization, so that starting polymeric structures with as little bias as possible have been built. For the PLA polymer two structures were prepared, considering the tacticity (*cis* or *trans*) of the chains. The structures were cleaned and optimized again by using PCFF molecular potential and the Conjugate gradient method. This minimization is inevitable for the subsequent molecular dynamics, because the velocities of atoms are computed based on the forces acting on each atom. If an overlap of atoms occurred at the constructed molecule, the movements of the atoms could be biased energetically.

Next, the equilibrium conformers of the polymeric structures were obtained by employing the molecular dynamics method with full atom model using the realistic PCFF potential. The equilibrium conformer represents a conformation fluctuating around a global potential energy minimum within an energy window corresponding to the thermal energy at the given temperature. The structures were equilibrated in the microcanonical ensemble employing Andersen method [44]. At the beginning of the simulation run the atoms were attributed to the Boltzmann distribution of velocities corresponding to the given temperature. Then the simulation runs for 1 ns of simulation were performed. At first, the simulations were performed at 400 K to enhance the conformational transitions. These 1 ns simulation runs were repeated until the potential energy of the system was observed to fluctuate around a constant value. Next, the system was thermalized to the room temperature (298 K) for 500 ps. Afterwards, data acquisition took place by saving atomic coordinates of the structures every 1 ps during a 100 ps production run. Thus, obtaining 100 structures for calculations of lengths of the building units in polymers was possible in this way. The obtained static pictures of the obtained equilibrium conformations have been visualized and discussed.

3. Results and discussion

3.1. Synthesis

Telechelic and star-shaped poly(ε-caprolactone)s with terminal hydroxyl groups were prepared via the controlled ring-opening polymerization of ε-caprolactone in THF using tin octoate ($Sn(Oct)_2$) as a catalyst and a corresponding polyol as a co-initiator (**ROH**) (Scheme 1). In the case of **APCL-6**, the DPET co-initiator was used in excess due to its partial insolubility in THF. It has recently been shown [18–22,35,45] that the actual initiator in the monomer/$Sn(Oct)_2$/**ROH** system is tin(II) alkoxide formed in the carboxylate-alkoxide ligand exchange reaction. Thus molar masses of polymers could be easily controlled by the initial $[M]_0/[\mathbf{ROH}]_0$ ratio and monomer conversion. All prepared polymers were characterized by SEC with refractive index detection and ^{1}H NMR spectroscopy (see Table 1). Except **APCL-4**, where the molar mass was slightly lower than theoretical value, the molar masses of the prepared polymers were in a good agreement with theoretical values confirming that the ring-opening polymerization process of ε-caprolactone was well controlled. Similarly ^{1}H NMR spectra of the prepared telechelic and star-shaped PCLs were consistent with the expected structure and confirmed the proposed mechanism of the initiation of polymerization as recently described for star-shaped poly(L-lactides) [35].

Esterification of the terminal –OH group of polymers with the pyrene based acyl chloride was used to functionalize the polymers with fluorescence probes. Reactions were carried out in pyridine, used both as a solvent and scavenger of HCl according to the published procedures [35,45]. In order to correctly interpret the data from static and especially from time-resolved fluorescence measurements, it was important that the hydroxyl group of each arm was functionalized with a pyrene label [46]. In the representative ^{1}H NMR spectra of 2- and 4-arm PCL (Fig. 1), in addition to signals attributed to the main-chain protons (signals **a**, **b**, **c**, **d**, **e** from repeating ε-caprolactone monomer unit), the signals related to the hydroxylic co-initiator (signals **f**, **g** for **APCL-2-PB** as well as **g′**, **h** and **i** in the case of **APCL-4-PB**) and pyrene-butyl group (**j**, **k**, **l**) with end protons of pyrene (**m**) were clearly detected (Scheme 2). Disappearance of signals of terminal –OH and caprolactone –C**H**$_2$–OH protons of non-functionalized polymer at 3.63–3.66 ppm in ^{1}H NMR spectra of functionalized polymers was clear evidence that the esterification of the hydroxyl end groups was completed. Molar masses of the functionalized polymers calculated from ^{1}H NMR spectra are shown in Table 2.

3.2. Fluorescence static measurements

A dilute THF solution of linear as well as star-shaped pyrene-functionalized PCLs exhibited absorption and emission spectra in the region typical for monosubstituted pyrene derivatives (Fig. 2). A calibration curve of dependence of absorbance on concentration of a model pyrene compound ethyl 4-(1-pyrene)butanoate in THF was used to calculate the molar masses of the prepared functionalized polymers from UV spectra of 1 wt% THF solutions of the polymers. The calculations were performed by extrapolation according to Lambert–Beer's law and the molar mass values are listed in Table 2. As seen from Table 2, except **APCL-6-PB**, the molar masses calculated from the UV spectra are in good agreement with molar masses calculated from ^{1}H NMR spectra supporting the quantitative functionalization of the polymers.

The absorption and emission parameters obtained from UV and static fluorescence measurements are listed in Table 3. Monomer emission of pyrene in the region 377–420 nm with partially resolved vibronic structure consists of four bands. In our

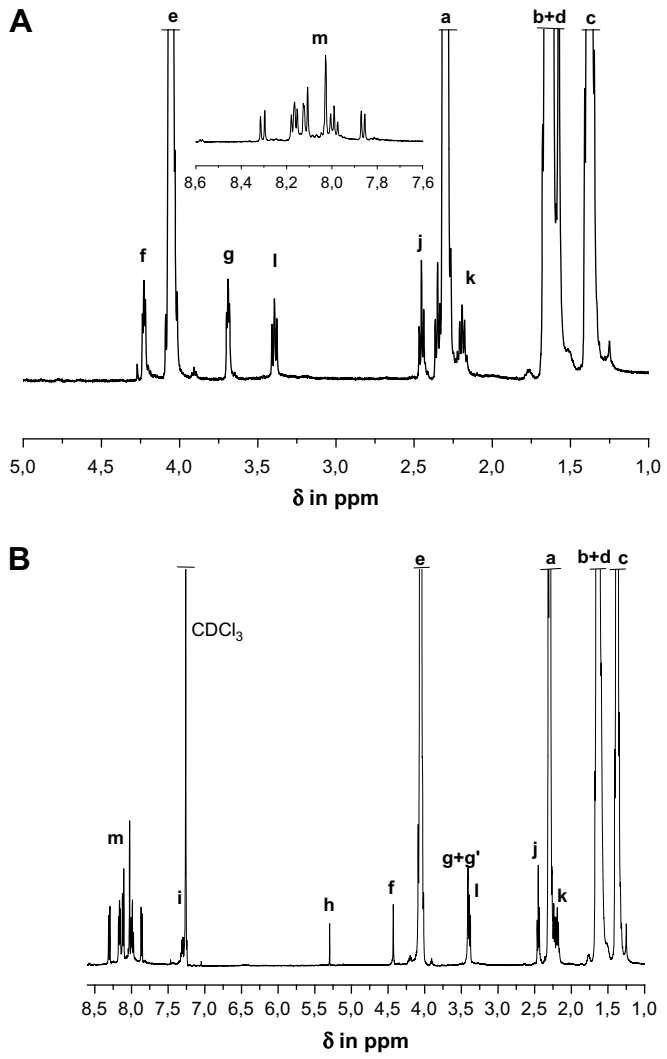

Fig. 1. ^{1}H NMR spectrum of telechelic **APCL-2-PB** (A) and 4-arm **APCL-4-PB** (B) polymers with pyrene-functionalized chain ends. The extent of functionalization of polymer terminal –OH groups with pyrene chromophore was calculated from $\mathbf{H_j/H_f}$ proton integrals ratio. Region 3.63–3.66 ppm shows absence of terminal –C$\mathbf{H_2}$–OH protons.

experimental arrangement with excitation and emission slits at 2.5 or 5 nm the second emission band at 383 nm was not visible (Fig. 2). Telechelic (**APCL-2-PB**) as well as star-shaped PCLs (**APCL-4-PB** and **APCL-6-PB**) showed also a broad band of excimer emission centered at 475 nm. The intensity of the excimer emission of all these polymer solutions did not depend on the concentration when measuring a pyrene chromophore concentration range of 10^{-8} to 10^{-6} M. The I_E/I_M values were within experimental error ±10% (Table 3, data for **APCL-2-PB** and **APCL-4-PB** are not shown).

This suggests that pyrene excimers are formed by intramolecular processes, similar to what was observed for star-shaped

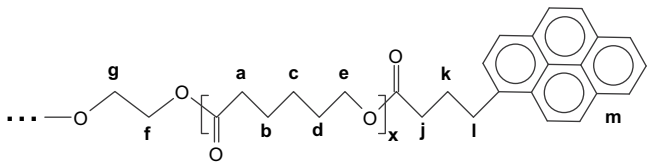

Scheme 2. Structure of functionalized dipyrenyl (2-arm) PCL polyester prepared using di(ethylene)glycol as the co-initiator for the polymerization with **H** protons corresponding to protons in ^{1}H NMR spectrum in Fig. 1.

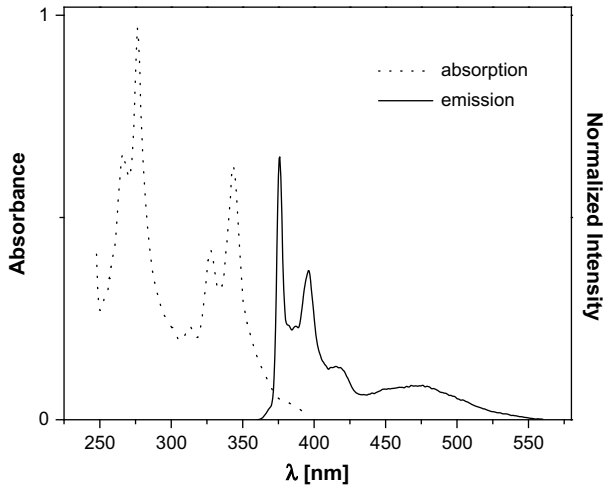

Fig. 2. Absorption and emission spectra of 6-arm PCL (**APCL-6-PB**) measured in THF at 25 °C at pyrene concentration of 10^{-6} mol L^{-1}. Excitation wavelength was 342 nm.

PLA in THF [35]. The excimer intensity increased with the increase in the number of polymer arms (see Table 3 and Fig. 3) as we showed for star-shaped PLA. However, while the I_E/I_M values determined for telechelic and 4-arm PCLs were comparable with those found for PLA star-shaped polymers, the I_E/I_M value determined for 6-arm PCL was lower than for PLA (see Fig. 3).

This is in contrast with the higher probability of end-to-end collision (formation of excimer) expected for more flexible PCL chains (more flexible ε-caprolactone structural unit). Another difference between these two polyesters is that the length of polymer chains for the same molar mass is not identical. These two reasons could be a possible explanation for the observed results. Generally, the pyrene excimers in good solvent are formed easier if the distance between pyrene chromophores is shorter [47,48]. Roughly estimating from the contribution of the atoms of monomers to the backbone of polymers PLA arms were about 16% shorter than PCL arms with the same average M_n, which could have led to above-mentioned effect on the higher excimer intensity [34,35,45,46,49,50]. However, these suggestions can be valid only on the assumption, that THF is good solvent for both polyesters and at the measured temperature both polymers have a similar extended coil conformation where polymer arms do not interact by any attractive interactions along the chain.

Excitation spectra performed for the monomer emission (375 nm) and for the excimer (475 nm) emission could bring deeper information about the formed excimers. When pyrene dimers are present in solution before the excitation, its excitation spectrum should be shifted to longer wavelengths than the spectrum recorded for the monomer emission.

The formation of pre-aggregated pyrene dimers or formation of dynamic excimers proceeds by well-known processes (Scheme 3). The longest-wavelength band of linear **APCL-2-PB** polymer with two linked pyrenes at the both ends recorded at the excimer emission 475 nm does not superpose the bands of excitation spectra recorded at the monomer emission (Fig. 4A). This unexpected result, from the point of view of comparison with similar functionalized poly(L-lactide), confirms the presence of pyrene dimers (static excimers) before the excitation. The magnitude of shifts of the longest-wavelength bands is about 1 nm, which is in agreement with that previously reported for aggregated ground-state pyrene present in solution of pyrene-modified (hydroxypropyl)cellulose [30,31], poly(ethyleneimine) [32] and poly(propyleneimine) dendrimer [51].

Table 3
Spectral parameters of PCL polymers from UV, emission and excitation spectra.

Polymer	No. of arms	c (polym.) [mol L^{-1}]	c (pyrene) [mol L^{-1}]	λ_{abs}[a] [nm] (log ε)	λ_{em}[b] [nm]	λ_{max}[c] (exc) [nm]		I_E/I_M
						M	E	
APCL-1-PB	1	5×10^{-8}	5×10^{-8}	342 (4.6103)	377, 386, 396, 416	342	–	0.01
APCL-2-PB	2	2.5×10^{-8}	5×10^{-8}	342 (4.9759)	376, 387, 396, 416, 475 (wide)	342	343	0.059
APCL-4-PB	4	1.3×10^{-8}	5×10^{-8}	342 (5.2539)	376, 387, 396, 416, 475 (wide)	342	342	0.115
APCL-6-PB	6	8.3×10^{-9}	5×10^{-8}	342 (5.6123)	376, 386, 397, 414, 475 (wide)	342	342	0.143
		1.7×10^{-8}	10^{-7}			–	–	0.137
		1.7×10^{-7}	10^{-6}			–	–	0.129

[a] The longest-wavelength band maximum; UV spectra were recorded in THF as a solvent at polymer concentration equal to 10^{-6} mol L^{-1}.
[b] The wavelength positions of emission maxima were the same in all measured concentration ranges.
[c] The longest-wavelength band maxima from excitation spectra monitored for monomer (M) and excimer (E) emission.

Recently, a similar observation was made for PCL polymers also by Martinho and co-workers [33]. They showed formation of stable polymer globules in THF below 0 °C in pyrene-labeled PCL at both ends with a molar mass ~19 200 g mol^{-1}. Above this temperature, the polymer adopted an extended coil conformation. The mentioned polymer can be compared with our dipyrene **APCL-2-PB**. Despite the molar masses not being comparable, we can expect similar behaviors for both polymers. In the excitation spectra as well as in the fluorescence decay profiles, the authors observed pyrene dimers and formation of static excimers without any rise-time component in the decay profile recorded for excimers at 520 nm. As an explanation, the authors reported hydrophobic interactions between chain-end pyrenes of linear polymer in THF even at the concentration of 10^{-6} mol L^{-1}. Contrary to that, our star-shaped 4- and 6-arm PCL polymers in THF did not exhibit the shift in excitation spectra (Fig. 4B). This suggests that there was no formation of static dimers of pyrene ends. Increasing the number of the polymer arms joined together in one point restricts such formation of the hydrophobic domain in a star polymer molecule.

3.3. Analysis of fluorescence decays

Additional information to the star-shaped PCL/THF system, apart from the static fluorescence measurements, should provide time-resolved fluorescence spectroscopy. Time profiles of the fluorescence intensity of pyrene-functionalized star-shaped PCLs were recorded by monitoring the monomer and excimer emission at 400 nm and 500 nm respectively. The decay curves for monomer and excimer emission of pyrene-functionalized six-arm PCL (**APCL-6-PB**) are shown in Fig. 5. Table 4 summarizes the corresponding data from fluorescence decay fits obtained for all prepared pyrene-functionalized polymers.

Fluorescence lifetime of pyrene-labeled PCLs was very effectively quenched by oxygen present in aerated THF, similarly we observed this for pyrene-functionalized star-shaped PLA [35]. Lifetime of the excited state of pyrene as well as the intensity of the fluorescence for **APCL-1-PB** in air saturated solution is about 10 times lower ($\tau = 24$ ns) than that found for degassed THF solution ($\tau = 210$ ns). However, after degassing of the THF solution, the bimolecular dynamic quenching with a rate constant in the range 10^{10} mol^{-1} L s^{-1} was observed. For this reason samples for time-resolved measurements were carefully degassed and sealed under vacuum using cells equipped with Teflon stopcock by a freeze–pump–thaw technique (at least 5 cycles). Only this technique ensured sufficiently low oxygen level, allowing reproducible results to be obtained. Thus for the linear **APCL-1-PB** polymer as a model, the monopyrenyl derivative, which has no possibility of the intramolecular excimer formation at least within the measured concentration range, the experimental decay monitored at 500 nm was monoexponential, as expected. On the other hand, complex fluorescence decays were obtained for the probes **APCL-2-PB**, **APCL-4-PB** and **APCL-6-PB** measured at the same molar concentration of pyrene (the molar concentrations of polymers were two, four, and six times lower, respectively). While the intensity of monomer fluorescence at various time points after excitation ($I_M(t)$) can be analyzed as a sum of two exponentials (equation (1)),

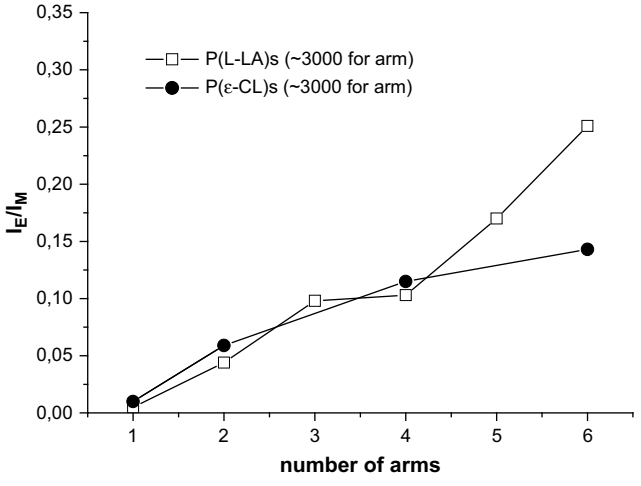

Fig. 3. Comparison of I_E/I_M ratio as a function of number of arms for star-shaped PCLs and PLAs with comparable length of arms (≈3000 g mol^{-1}) measured in THF at 25 °C at pyrene concentration of 5×10^{-8} mol L^{-1}.

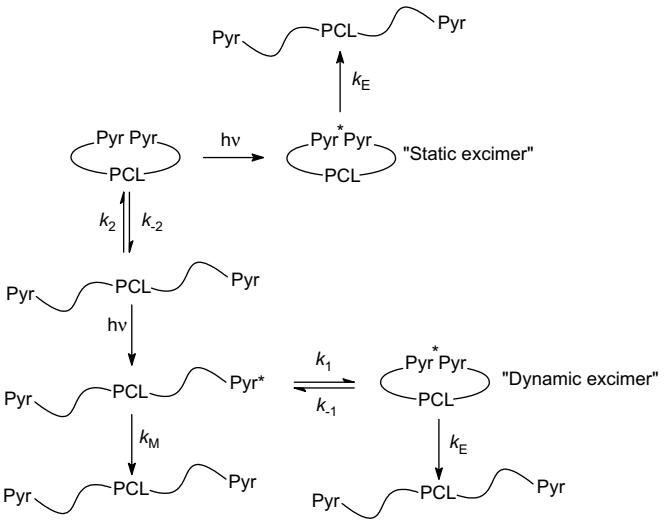

Scheme 3.

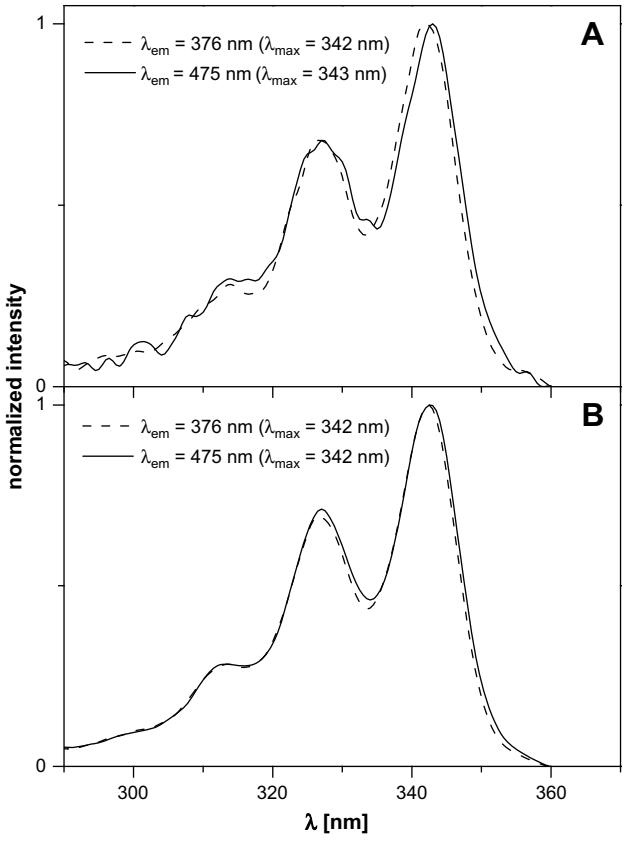

Fig. 4. Normalized excitation spectra of telechelic (2.5×10^{-8} mol L^{-1} solution) (A) and 4-arm (2.5×10^{-7} mol L^{-1} solution) PCLs (B) as an example of star-shaped polymers in THF at 25 °C monitored at monomer and excimer emission.

a reasonable fit to the excimer fluorescence data ($I_E(t)$) is only possible with sum of three exponentials (equation (2), Table 4). The third component provides analysis for the formation of excimers occurred during the lifetime of excited state of pyrene.

$$I_M(t) = A_1 \exp(-t/t_1) + A_2 \exp(-t/t_2) \quad (1)$$

$$I_E(t) = A_1 \exp(-t/t_1) + A_2 \exp(-t/t_2) + A_3 \exp(-t/t_3) \quad (2)$$

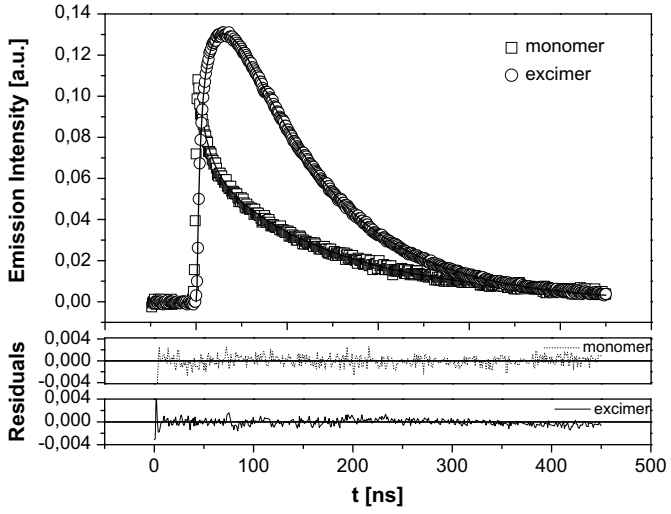

Fig. 5. Fluorescence decay profiles of **APCL-6-PB** polymer for monomer and excimer recorded at 400 nm and 500 nm, respectively, measured in THF at 25 °C at concentration of 10^{-6} mol L^{-1}.

Tri-exponential kinetics of excimer decay with two negative and one positive component were observed for telechelic as well as 4- and 6-arm PCLs. For comparison in the case of star-shaped PLAs [35] the polymers with a higher number of arms (5 and 6) had kinetics represented with two positive pre-exponential factors as a consequence of a formation of two distinguished excimers while polymers with a lower number of arms (2 and 3) had kinetics of excimer decay with two negative factors, similarly to what was observed here for both ditelechelic and star-shaped PCLs. In the case of 4-arm PLA, the excimer emission pattern was fitted with four exponentials with two negative and two positive pre-exponential factors. Two possible explanations: (1) a formation of static excimers or (2) an interaction of pyrene ends with benzyl groups in a core (in the case of 5- and 4-arm PLAs with one and two hydroxyl groups of DPET, respectively, blocked by benzyl groups) were already discussed [35]. On the other hand, reasonable fit with three exponentials obtained here for the star-shaped PCLs suggests different behaviors of PCL stars (with regard to PLA stars) in THF solution. One possible explanation based on the different length of PCL and PLA arms (the same molar mass but different arm length) was already discussed above in static measurements part. Another possible explanation, supported below by molecular dynamic simulations is a different conformation of the star-shaped PLAs compared to star-shaped PCLs. In the shape of those branched molecules with m-DPET core (see Scheme 1), PLA arms probably distinguish the position of pyrene on a different side of the molecule and formed excimers that are not topologically equal. In mathematical expressions we therefore have four components with two monomers M(1)* and M(2)* as well as with two excimers D(1)* and D(2)* [35]. On the other hand, PCL arms are more flexible and do not 'feel' such a steric hindrance.

More detailed studies of time-resolved fluorescence of star-shaped PCLs showed that the corresponding decay curves for **APCL-6-PB** were found to be independent of the measured concentration within a concentration range of 10^{-6} to 10^{-4} mol L^{-1}. This observation indicated that in the THF solution the excimers were formed by intramolecular interactions of pyrenes, supporting results from the static fluorescence measurements. On the other hand, from time-resolved fluorescence spectroscopy ditelechelic **APCL-2-PB** (in agreement with excitation spectra) and 4-arm **APCL-4-PB** showed a small extent of formed pyrene dimers before excitation (static excimers), while a rise-time component was clearly seen on their decay traces attributed to dynamic formation of excimers (Fig. 6). Fig. 7 shows the time-resolved fluorescence spectra of **APCL-4-PB** (10^{-6} mol L^{-1}) in THF recorded at different delays after reaching the maximum intensity of a laser excitation pulse. The nanosecond time scale spectra can be analyzed by a superposition of three components: pyrene monomer emission (with vibrational peaks at 376–419 nm); structureless band at 435 nm and a classical excimer band at 470–480 nm. The blue-shifted excimer vanishes at longer time range. This emission can be assigned to excimers with only partial overlap of the pyrene moieties, by analogous with pyrene-labeled (hydroxypropyl)cellulose in water [52]. The spectrum recorded after 90 ns corresponded well to the steady-state fluorescence spectrum recorded for the studied solution.

According to the Zachariasse model [53], star-shaped polymers with pyrene-functionalized ends are imaged as α,ω-bipyrenyl linear structures [35] and can be used to evaluate the ratio of the sum of negative and positive pre-exponential factors of the decay curves (Table 4). The ratio equals to −1 if the excimer formation is diffusion controlled, or equals to 0 if a direct excitation of pyrene aggregates proceeds. As seen from Table 4 the corresponding ratio values are between −0.5 and −1 suggesting that additional fluorescence species, which emit in the same area where pyrene excimers emit, were formed only partially and their amount decreases with

Table 4
Parameters of pyrene-functionalized star-shaped PCLs as determined by fitting of experimental fluorescence decay curves and ratio of negative and positive pre-exponential factors for excimer emission from equation (2).

Polymer	Monomer		Excimer			A_{E-}/A_{E+}
	τ_1 [ns] (A_1)	τ_2 [ns] (A_2)	τ_1 [ns] (A_1)	τ_2 [ns] (A_2)	τ_3 [ns] (A_3)	
APCL-1-PB	210					–
APCL-2-PB	9.96 (0.054)	188.6 (0.278)	7.14 (−0.040)	28.26 (−0.015)	159.04 (0.096)	−0.68
APCL-4-PB	30.31 (0.135)	144.3 (0.198)	5.93 (−0.058)	36.87 (−0.322)	115.44 (0.523)	−0.73
APCL-6-PB	12.11 (0.041)	135.8 (0.066)	3.43 (−0.099)	24.5 (−0.13)	101.97 (0.2275)	−1.01

τ – fluorescence lifetime of excited state of pyrene.
A_x – pre-exponential factors.
A_{E-} – sum of negative pre-exponential factors.
A_{E+} – sum of positive pre-exponential factors.

an increase in the number of arms of star-shaped PCLs. Since the ratio of pre-exponential factors for **APCL-6-PB** is almost equal to −1, it seems that the star-shaped structure with 6 or more arms prevents static end-to-end pyrene interactions. As a conclusion, postulated also for star-shaped PLAs [35], the reported fluorescence studies indicate that in the case of macromolecules containing lower number (i.e. two or four) of arms there is enough space for free dynamics of arm segments allowing formation of static pyrene excimers in the interior of the star-shaped PCLs. On the other hand, due to higher steric hindrance in the case of star-shaped PCLs with more than six arms, the chain-end pyrenes are located mostly at the periphery of the star-shaped macromolecules. As intuitively expected for other star-shaped polymers, increasing the number of arms in one macromolecule leads to their stretching away from the center of the macromolecule.

The measured decay profile of the **APCL-2-PB** polymer was substantially different from the mentioned decay profile of bipyrenyl telechelic PCL showed by Martinho et al. [33]. The authors observed for the decay obtained at a temperature of −10 °C, only a complex decay profile fitted with the sum of four exponentials with a very short rise-time component. It was evident, that the length of polymer and distance of the two pyrene chromophores linked at each end were responsible for the differences measured for both marked PCL polymers. In the case of PCL with a molecular weight ≈19 200 g mol^{-1} formation of dynamic excimers was suppressed and it was possible the polymer reached a globular structure, where pyrenes were entrapped closer to each other.

3.4. Molecular simulations

In order to provide an additional support for our interpretations of the florescence measurement results, molecular simulations of monomers ε-caprolactone monomer or L,L-dilactide as well as their derived 6-arm PCL and PLA star-shaped polymers have been performed. The molecular simulations started from "sketch", and the constructed structures were several times optimized according to the standard procedure described in the Experimental section, in order to avoid obtaining biased conformations. Additionally, in the case of the monomer structures, geometries have been optimized by using the semi-empirical quantum mechanics method, which represented optimal level of theory from the aspect of computational costs for this problem. In the applied models for our molecular simulations the molecules were held in vacuum and no solvent effects were considered. Including the explicit solvent molecules into model would increase the computational size of the system, mainly due to tens thousands of solvent atoms necessary in the case of polymeric structures. The computational size could be reduced by a group model for molecular potential function of solvent. Nevertheless, the computational expenses would be behind the framework of this primary experimental work.

First of all, the geometrical characteristics of monomers, corresponding to the building units, were computed and summarized in Table 5. The largest volumes were calculated for the central (core) DPET monomer and the ending 4(1-pyrene)butanoyl unit. On the other hand the volumes of the repeating units were very similar,

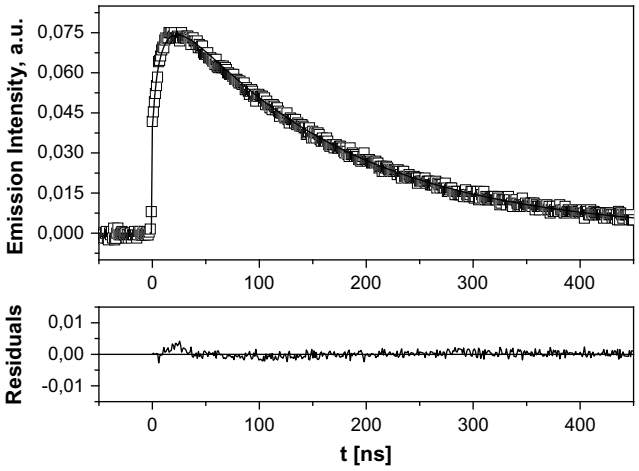

Fig. 6. Fluorescence decay profiles of **APCL-2-PB** polymer excimer recorded at 500 nm, measured at a concentration of 10^{-6} mol L^{-1} (calculated for pyrene) in THF at 25 °C and corresponding mathematical fitting.

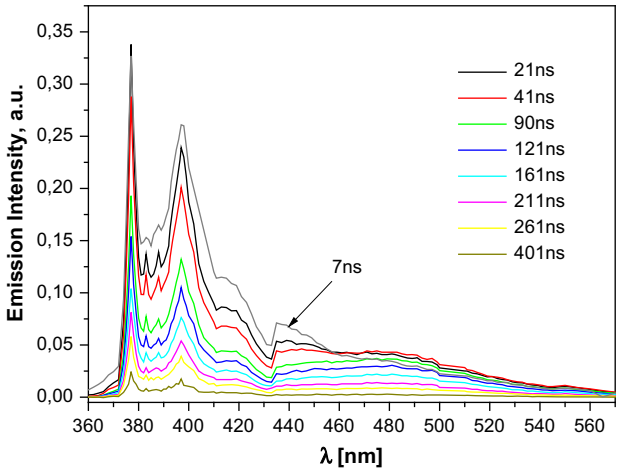

Fig. 7. Transient emission spectra of **APCL-4-PB** monitored at different time after excitation at 337 nm. Measurement was performed in THF solution at 25 °C at concentration of 10^{-6} mol L^{-1} (calculated for pyrene).

Table 5
Geometry of monomers corresponding to the building units.

Unit	N	M_w [g mol^{-1}]	L_X [Å]	L_Y [Å]	L_Z [Å]	A [Å^2]	V [Å^3]	A_S [Å^2]	V_S [Å^3]
Center	33	248.2309942	11.421	7.519	6.609	285.800	225.216	433.8	718.5
Ending	36	271.3389934	15.302	9.638	4.215	298.195	255.611	493.7	807.8
MU1	18	114.1439974	10.612	5.277	4.275	166.001	119.513	314.3	452.7
t-MU2	18	144.1259966	9.025	6.944	5.476	177.001	131.258	328.5	482.9
c-MU2	18	144.1259966	9.432	6.325	6.177	176.246	131.220	332.2	484.0

Center – di(pentaerythritol); ending – 4-(1-pyrene)butanoyl; MU1 – ε-caprolactone; MU2 – L,L-dilactide; N – number of atoms; M_w – exact mass; L_X – length; L_Y – height; L_Z – width; A – van der Waals surface; V – van der Waals volume; A_S – solvent accessible area ($R_S = 1.4$ Å); V_S – solvent excluded volume ($R_S = 1.4$ Å).

differing by ~10% as computed for van der Waals radii of atoms. Additionally, also the so-called solvent excluded volumes of the units were calculated. These volumes represent the volume "as seen" by molecular bodies. A typical solvent radius in this calculation was set to $R_S = 1.4$ Å as an average of the atomic radii present in the system. Here we can observe that the difference between the volumes V_S diminishes to ~5% implying that the building units should have a similar steric hindrance effect. Furthermore, the computed dimensions L_i correspond to axes of ellipsoid circumscribing a given monomer. The major axis corresponding to the length of the monomer implies a longer length of the PCL building units. The relationship of axes $L_Y < L_Z$ indicates flat-shaped geometries of the core and ending units, while the building units are rather symmetric $L_Y \leq L_Z$.

In the following, the polymeric structures 6-arm PCL and PLA star-shaped polymers have been constructed. In this stage, the optimized monomers were connected to each other with respect to hybridization, so that starting structures with as little bias as possible have been built. Based on the hybridization principle, two polymer structures with *cis*- and *trans*-tacticity have been constructed in the case of PLA. Next, the constructed structures were optimized by minimizing the potential energy in order to remove a possible bias in energy during the following MD simulation runs. At the end of the MD simulations equilibrium conformers together with 100 ps trajectory for analyses have been obtained, according to the procedural described in the Experimental section.

The coordinates of the structures of the production run after 100 ps were used for calculation of the distribution of lengths of the monomers (Table 6). As the length of the monomer, the distance between two backbone oxygens of ester groups ($2n$ in the case of L,L-dilactide (LA) monomer) was considered. Using this method the average lengths of CL and LA derived units were obtained. As we expected, the length of CL unit was about 11% longer (7.24 Å) than the length of LA derived unit (6.517 Å).

Moreover, the equilibrium conformer obtained by the MD simulations supported our previous interpretation that PLA arms aligned and intertwined while PCL forms a coil conformation. Fig. 8 shows an evolution of the structures through the different stages of the MD simulation, together with a "static" snapshot of the resulting conformation. The figure shows that, in the case of the PCL, the starting conformation after energy minimization became curlier, with respect to the sketch, while in the case of PLAs the starting structures are more or less preserved. This is most likely due to higher displacements within the energy minimization, signaling more flexible polymeric chains. The PCL's composition of more flexible segments was reflected also by the resulting globular conformation at the end of the MD simulations. Also it can be noteworthy that (particularly) in the case of the PLA with *trans* tacticity the arms of the starting polymeric structure were in helical conformation due to the hybridization. In the case of the "*cis*-PLA" the starting conformation is very similar to that of PCL. However at the end of the MD simulation both PLA polymers formed a very similar extended conformation with twisted arms. This suggests that the observed distinct conformer evolution between PCL and PLA is a result of rather strong intramolecular interactions and would not depend on starting structure. Although, the simulations were performed in vacuum and did not consider the effect of solvent as we mentioned earlier, the resulting equilibrium conformer exhibits a natural tendency of the PLA stars to form entangled and twisted conformations of their telechelic arms consistently with our previous observations based on experiments.

This difference could provide an explanation for the higher probability of the pyrene excimer formation in the case of PLA stars in comparison with PCL stars observed experimentally (see Fig. 3). It is well known, that polylactides with different optical activity – poly(L-lactide) with poly(D-lactide) – form stereocomplexes with a helical conformation, where chains are twisted as a consequence of hydrogen bonding between carbonyl oxygen and side methyl protons multiplied many times by interactions along polymer chains [54,55]. According to the molecular simulations of Brizzolara [54] two poly(L-lactide) chains can also interact together and form helix structure. The structure obtained on the basis of the presented herein MD simulations, visualized in Fig. 8, shows similar interactions of polymer arms in star PLAs with terminal pyrenes. In such conformation the excimers can be formed easier than in the case of PCL stars. Thus the molecular modeling, presented here, complements our previous theory that 5- and 6-arm PLA stars with terminal pyrenes form two different excimers clearly seen from fluorescence decay data presented in our recent work [35]. On the basis of molecular modeling, there are two different dominant conformations of the chains in 6-arm PLA star. It is worth to note that for one conformer only a small rearrangement of the polyester chain is required to form the excimer, whereas in the second conformer, the distance and orientation of the terminal pyrene units are less convenient to assume a sandwich structure.

In contrast to PLA stars, PCL stars form a polymer conformation with a more random coil characteristic. This is due to the higher flexibility of the polymer together with the larger length of PCL chains. The excimers in PCL stars are then formed statistically. This is supported also by the experimental excimer decay profile, where two pre-exponential factors are negative and one positive. This suggests that, in the case of PCL stars, only one type of excimers is formed.

In conclusion, we showed the differences in solution behaviors between star-shaped polyesters such as PLA and PCL using fluorescence spectroscopy. All chain-end groups of the mentioned polymers were fully functionalized with pyrene, used as a fluorescence probe. Static as well as time-resolved fluorescence measurements showed formation of pyrene excimer as

Table 6
Average distances of two backbone oxygens of monomer unit in PCL and PLA polymer arms calculated for 6-arm star-shaped polymers.

Monomer	Minimal length [Å]	Maximal length [Å]	Average length [Å]	Standard deviation [Å]
ε-Caprolactone	6.316	7.671	7.240	0.228
L,L-Dilactide *trans*-tacticity	5.345	7.786	6.517	0.370
L,L-Dilactide *cis*-tacticity	5.338	7.680	6.665	0.390

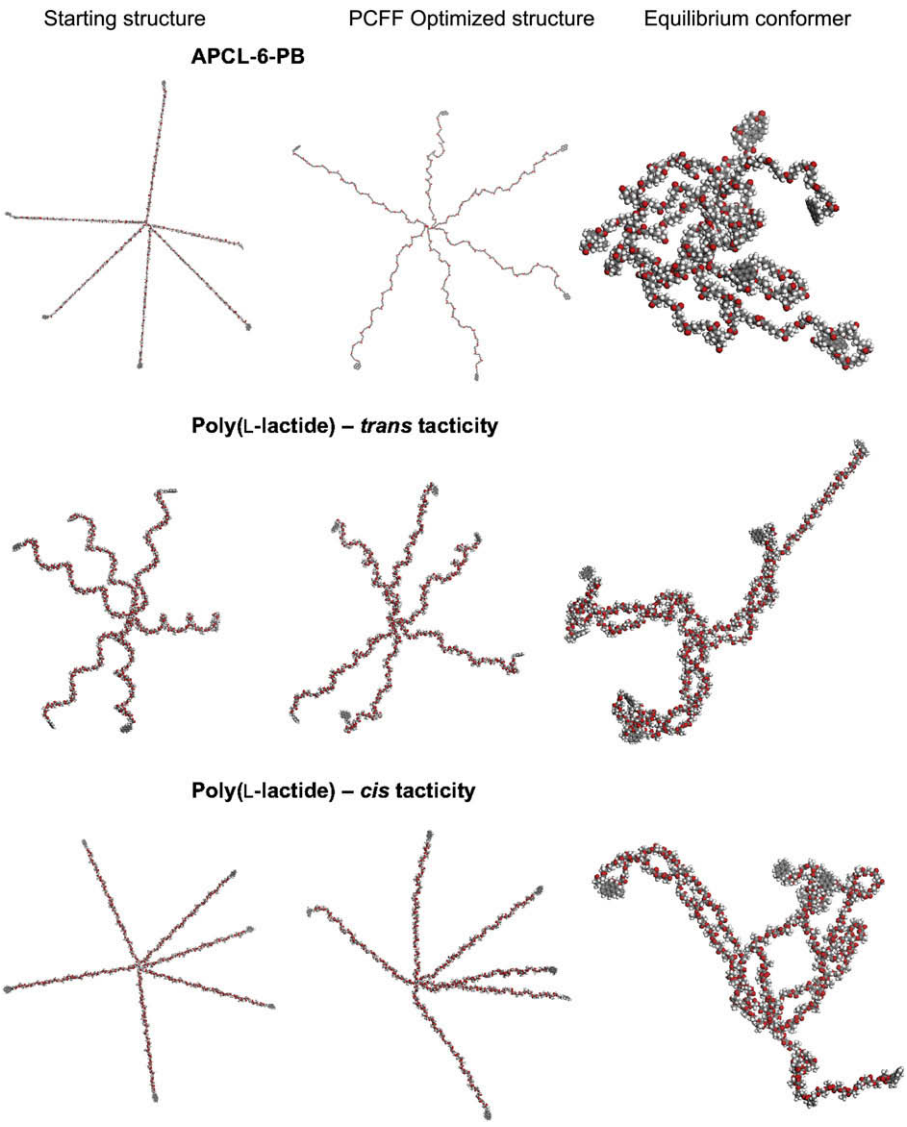

Fig. 8. Three stages of the molecular simulations: sketch, optimization and MD of 6-arm star-shaped PCL and PLAs constructed of di(pentaerythritol) core, 20 monomer units of ε-caprolactone or L,L-dilactide per one polyester arm and terminal 4-(1-pyrene)butanoyl moiety at each chain end exhibit a natural tendency of the PLA stars to form entangled and twisted conformations of their telechelic arms.

a consequence of chain end interaction in THF. In dipyrene–telechelic PCL, partial formation of static excimers was observed probably due to hydrophobic interaction of the pyrene moieties. Such interactions were not observed for star-shaped 4- or 6-arm polyesters. 6-Arm PCL star exhibited lower extent of excimers than similar (with respect of M_n for single arm) 6-arm PLA star. Moreover, excimers in PCL star were formed in slightly a different manner than excimers in PLA star-shaped polyesters as supported by molecular simulations which helped for better understanding of results from time-resolved fluorescence measurements.

Acknowledgement

The authors thank for support of the Polish Ministry of Scientific Research and Higher Education – grant no. PBZ-MNiSW-01/II/2007. Dr. M. Danko is thankful for the financial support of the European Commission within the 5th Framework Program – Contract ICA1-CT-2000-70021 – Center of Excellence (administered by Polish Academy of Sciences), VEGA grant agency of Slovak Republic through grant Nos. 2/0097/09, 2/0082/08 and APVV grant agency for the financial support of this work through projects No. 003206 and 51-004904.

References

[1] Perrin DE, English JP. In: Domb AJ, Kost J, Wiseman DM, editors. Handbook of biodegradable polymers. Amsterdam: Harwood Academic Publishers; 1997 [chapter 3].
[2] Pitt CG. In: Chasim M, Langer R, editors. Biodegradable polymers as drug delivery systems. New York: Marcel Dekker; 1990 [chapter 3].
[3] Holland SJ, Tighe BJ, Gould PL. J Control Release 1986;4(3):155–80.
[4] Matyjaszewski K, Gnanou Y, Leilbler L. Macromolecular engineering: precise synthesis, material properties, applications. Weinheim: Wiley-VCH Verlag GmbH & Co. KGaA; 2007.
[5] Mecerreyes D, Jerome R, Dubois P. Adv Polym Sci 1999;147:1–59.
[6] Stridsberg K, Ryner M, Albertsson A-Ch. Adv Polym Sci 2002;157:41–65.
[7] Duda A, Penczek S. Mechanism of aliphatic polyester formation. In: Steinbuechel A, Doi Y, editors. Polyesters II – properties and chemical synthesis. Biopolymers, vol. 3b. Weinheim: Wiley-VCH; 2002. p. 371.
[8] Dong CM, Qiu KY, Gu ZW, Feng XD. J Polym Sci Part A Polym Chem 2002;40(3):409–15.
[9] Lee SH, Kim SH, Han YK, Kim YH. J Polym Sci Part A Polym Chem 2001;39(7):973–85.
[10] Kim ES, Kim BC, Kim SH. J Polym Sci Part A Polym Chem 2004;42(6):939–46.
[11] Korhonen H, Helminen A, Seppala JV. Polymer 2001;42(18):7541–9.

[12] Finne A, Albertsson AC. Biomacromolecules 2002;3(4):684–90.
[13] Zhao YL, Cai Q, Jiang J, Shuai XT, Bei JZ, Chen CF, et al. Polymer 2002;43(22):5819–25.
[14] Cai Q, Zhao Y, Bei J, Xi F, Wang S. Biomacromolecules 2003;4(3):828–34.
[15] Biela T, Duda A, Penczek S, Rode K, Pasch H. J Polym Sci Part A Polym Chem 2002;40(15):2884–7.
[16] Biela T, Duda A, Rode K, Pasch H. Polymer 2003;44(6):1851–60.
[17] Klok HA, Becker S, Schuch F, Pakula T, Muellen K. Macromol Biosci 2003;3(12):729–41.
[18] Kowalski A, Duda A, Penczek S. Macromol Rapid Commun 1998;19(11): 567–72.
[19] Kowalski A, Duda A, Penczek S. Macromolecules 2000;33(3):689–95.
[20] Kowalski A, Libiszowski J, Duda A, Penczek S. Macromolecules 2000;33(6): 1964–71.
[21] Kowalski A, Duda A, Penczek S. Macromolecules 2000;33(20):7359–70.
[22] Majerska K, Duda A, Penczek S. Macromol Rapid Commun 2000;21(18): 1327–32.
[23] Yuan W, Zhu L, Huang X, Zheng S, Tang X. Polym Degrad Stab 2005;87(3): 503–9.
[24] Yuan W, Tang X, Huang X, Zheng S. Polymer 2005;46(5):1701–7.
[25] Huang H-X, Yang K-K, Wang Y-Z, Wang X-L, Li Y. J Polym Sci Part A Polym Chem 2006;44(3):1245–51.
[26] Hecht S, Ihre H, Frechet JMJ. J Am Chem Soc 1999;121(39):9239–40.
[27] Hecht S, Vladimirov N, Frechet JMJ. J Am Chem Soc 2001;123(1):18–25.
[28] Atthoff B, Trollsas M, Claesson H, Hedrick JL. Macromol Chem Phys 1999;200(6):1333–9.
[29] Radke W, Rode K, Gorshkov AV, Biela T. Polymer 2005;46(15):5456–65.
[30] Winnik FM. Chem Rev 1993;93(2):587–614.
[31] Winnik FM, Winnik MA, Tazuke S, Ober CK. Macromolecules 1987;20(1): 38–44.
[32] Winnik MA, Bystryak SM, Liu Z, Siddiqui J. Macromolecules 1998;31(20): 6855–64.
[33] Picarra S, Gomes PT, Martinho JMG. Macromolecules 2000;33(10):3947–50.
[34] Cuniberti C, Perico A. Eur Polym J 1977;13(5):369–74.
[35] Danko M, Biela T, Libiszowski J, Wolszczak M, Duda A. J Polym Sci A Polym Chem 2005;43(19):4586–99.
[36] Biela T, Duda A, Rode K, Pasch H. J Polym Sci Part A Polym Chem 2005;43(23): 6116–33.
[37] Maple JR, Dinur U, Hagler AT. Proc Natl Acad Sci U S A 1988;85(15):5350–4.
[38] Polak E, Ribiere G. Rev Fr Inform 1969;16:35.
[39] Dewar MJS, Zoebisch EG, Healy EF, Stewart JJ. J Am Chem Soc 1985;107(13): 3902–9.
[40] Rocha GB, Freire RO, Simas AM, Stewart JJ. J Comput Chem 2006;27(10): 1101–11.
[41] Stewart JJ. MoPac2007, QCPE, Department of Chemistry, Indiana University.
[42] Connolly ML. J Am Chem Soc 1985;107(5):1118–24.
[43] Rohrbaugh RH, Jurs PC. Anal Chim Acta 1987;199:99–109.
[44] Andersen HC. J Chem Phys 1980;72(4):2384.
[45] Sosnowski S, Slomkowski S, Penczek S. Macromol Chem – Macromol Chem Phys 1991;192(7):1457–65.
[46] Ingratta M, Duhamel J. Macromolecules 2007;40(18):6647–57.
[47] Birks JB. Photophysics of aromatic molecules. New York: Wiley & Sons; 1970. p. 304.
[48] Hrdlovic P, Lukac I. J Photochem Photobiol A Chem 2000;133(1–2):73–82.
[49] Winnik MA, Redpath AEC, Richards DH. Macromolecules 1980;13(2):328–35.
[50] Winnik MA, Redpath AEC, Paton K, Danhelka J. Polymer 1984;25(1):91–9.
[51] Baker LA, Crooks RM. Macromolecules 2000;33(24):9034–9.
[52] Winnik FM, Tamai J, Yonezawa N, Nishimura Y, Yamazaki I. J Phys Chem 1992;96(4):1967–72.
[53] Zachariasse KA, Kuhnle W, Leinhos U, Reynders P, Striker G. J Phys Chem 1991;95(14):5476–88.
[54] Brizzolara D, Cantow H-J, Diederichs K, Keller E, Domb AJ. Macromolecules 1996;29(1):191–7.
[55] Biela T, Duda A, Penczek S. Macromolecules 2006;39(11):3710–3.